Discovery of TeV γ-ray emission from the neighbourhood of the supernova remnant G24.7+0.6 by MAGIC

MAGIC Collaboration, V. A. Acciari[1], S. Ansoldi[2,20], L. A. Antonelli[3], A. Arbet Engels[4], C. Arcaro[5], D. Baack[6], A. Babić[7], B. Banerjee[8], P. Bangale[9], U. Barres de Almeida[9,10], J. A. Barrio[11], J. Becerra González[1], W. Bednarek[12], E. Bernardini[5,13,23], A. Berti[2,24], J. Besenrieder[9], W. Bhattacharyya[13], C. Bigongiari[3], A. Biland[4], O. Blanch[14], G. Bonnoli[15], R. Carosi[16], G. Ceribella[9], A. Chatterjee[8], S. M. Colak[14], P. Colin[9], E. Colombo[1], J. L. Contreras[11], J. Cortina[14], S. Covino[3], P. Cumani[14], V. D'Elia[3], P. Da Vela[15], F. Dazzi[3], A. De Angelis[5], B. De Lotto[2], M. Delfino[14,25], J. Delgado[14,25], F. Di Pierro[5], A. Domínguez[11], D. Dominis Prester[7], D. Dorner[17], M. Doro[5], S. Einecke[6], D. Elsaesser[6], V. Fallah Ramazani[18], A. Fattorini[6], A. Fernández-Barral[5], G. Ferrara[3], D. Fidalgo[11], L. Foffano[5], M. V. Fonseca[11], L. Font[19], C. Fruck[9], D. Galindo[20]⋆, S. Gallozzi[3], R. J. García López[1], M. Garczarczyk[13], M. Gaug[19], P. Giammaria[3], N. Godinović[7], D. Guberman[14], D. Hadasch[21], A. Hahn[9], T. Hassan[14], J. Herrera[1], J. Hoang[11], D. Hrupec[7], S. Inoue[21], K. Ishio[9], Y. Iwamura[21], H. Kubo[21], J. Kushida[21], D. Kuveždić[7], A. Lamastra[3], D. Lelas[7], F. Leone[3], E. Lindfors[18], S. Lombardi[3], F. Longo[2,24], M. López[11], A. López-Oramas[1], C. Maggio[19], P. Majumdar[8], M. Makariev[22], G. Maneva[22], M. Manganaro[7], K. Mannheim[17], L. Maraschi[3], M. Mariotti[5], M. Martínez[14], S. Masuda[21], D. Mazin[9,21], M. Minev[22], J. M. Miranda[15], R. Mirzoyan[9], E. Molina[20], A. Moralejo[14], V. Moreno[19], E. Moretti[14], V. Neustroev[18], A. Niedzwiecki[12], M. Nievas Rosillo[11], C. Nigro[13], K. Nilsson[18], D. Ninci[14], K. Nishijima[21], K. Noda[21], L. Nogués[14], S. Paiano[5], J. Palacio[14], D. Paneque[9], R. Paoletti[15], J. M. Paredes[20], G. Pedaletti[13], P. Peñil[11], M. Peresano[2], M. Persic[2,26], P. G. Prada Moroni[16], E. Prandini[5], I. Puljak[7], J. R. Garcia[9], W. Rhode[6], M. Ribó[20], J. Rico[14], C. Righi[3], A. Rugliancich[15], L. Saha[11], T. Saito[21], K. Satalecka[13], T. Schweizer[9], J. Sitarek[12], I. Šnidarić[7], D. Sobczynska[12], A. Somero[1], A. Stamerra[3], M. Strzys[9], T. Surić[7], F. Tavecchio[3], P. Temnikov[22], T. Terzić[7], M. Teshima[9,21], N. Torres-Albà[20], S. Tsujimoto[21], G. Vanzo[1], M. Vazquez Acosta[1], I. Vovk[9], J. E. Ward[14], M. Will[9], D. Zarić[7];
and E. de Oña Wilhelmi[27,28,29]†, D. F. Torres[27,28,30], R. Zanin[31]‡,

(Affiliations can be found after the references)

13 December 2018

ABSTRACT

SNR G24.7+0.6 is a 9.5 kyrs radio and γ-ray supernova remnant evolving in a dense medium. In the GeV regime, SNR G24.7+0.6 (3FHL J1834.1–0706e/FGES J1834.1–0706) shows a hard spectral index (Γ~2) up to 200 GeV, which makes it a good candidate to be observed with Cherenkov telescopes such as MAGIC. We observed the field of view of SNR G24.7+0.6 with the MAGIC telescopes for a total of 31 hours. We detect very high energy γ-ray emission from an extended source located 0.34° away from the center of the radio SNR. The new source, named MAGIC J1835–069 is detected up to 5 TeV, and its spectrum is well-represented by a power-law function with spectral index of 2.74 ± 0.08. The complexity of the region makes the identification of the origin of the very-high energy emission difficult, however the spectral agreement with the LAT source and overlapping position at less than 1.5σ point to a common origin. We analysed 8 years of *Fermi*-LAT data to extend the spectrum of the source down to 60 MeV. *Fermi*-LAT and MAGIC spectra overlap within errors and the global broad band spectrum is described by a power-law with exponential cutoff at 1.9 ± 0.5 TeV. The detected γ-ray emission can be interpreted as the results of proton-proton interaction between the supernova and the CO-rich surrounding.

Key words: acceleration of particles – cosmic rays – ISM:supernova remnants – ISM: clouds – gamma-rays: general

1 INTRODUCTION

Composite supernova remnants (SNRs) are known to accelerate particles to very high energies (VHE), up to hundreds of TeV or beyond (Albert et al. 2007; Aleksić et al. 2012), in their expanding shocks and/or the relativistic wind surrounding the left-over, energetic pulsar. Both leptonic and hadronic non-thermal mechanisms produce γ-ray emission that extends from a few hundreds of MeV to tens of TeV. This radiation can be generated by the interaction of relativistic electrons scattering off low-energy photon fields, and/or by pion production and decay from direct inelastic collisions of ultrarelativistic protons with target protons of the interstellar medium (S. Longair 1992).

SNR G24.7+0.6 is a $0.5° \times 0.25°$ center-filled SNR located at a distance of ~5 kpc (Reich et al. 1984; Leahy 1989). It was discovered at radio frequencies as a couple of incomplete shells centered at $\mathrm{RA_{J2000}} = 278.57°$ and $\mathrm{DEC_{J2000}} = -7.09°$, and a linearly polarized central core with a flat radio spectrum of $\alpha = -0.17$ (Reich et al. 1984), indicating the presence of a central pulsar wind nebula (PWN) powered by an undetected pulsar. With an estimated age of 9.5 kyrs (Leahy 1989) it belongs to the class of middle-aged SNRs interacting with molecular clouds (MC) as suggested by observations in the infrared (IR) energy band and by the detection of ^{13}CO J=1-0 line at 110 GHz (Galactic Ring Survey, Jackson et al. 2006). Petriella et al. (2008, 2012) discovered several molecular structures, including a molecular arm extending into the center of the SNR and two clouds bordering the remnant. An observation using VLA also revealed several ultracompact H II regions within the SNR. The presence of many young stellar objects in the interaction region between the SNR and the MC (Petriella et al. 2010) also suggests that the large activity related to the SN in the region might be triggering stellar formation.

⋆
†
‡

In X-rays, the SNR was observed with the Einstein Observatory. Although not included in the Einstein catalog of SNRs (Seward 1990), Leahy (1989) derived a flux over the entire SNR region of $(3.9 \pm 0.9) \times 10^{-13}$ erg cm^{-2} s^{-1}. The same data yield an upper limit (UL) to a differential flux under the assumption of a point source (<2′ diameter) and extended (circle of 8′ radius) emission of $< 1 \times 10^{-12}$ erg cm^{-2} s^{-1} and $< 3 \times 10^{-12}$ erg cm^{-2} s^{-1}, respectively. No pulsar or PWN has been found yet, although an attempt was done with *XMM*-Newton (OBS. ID:0301880301, PI: O. Kargaltsev). Unfortunately, a strong flare in the field of view (FoV) affected the observation, reducing the useful exposure to only 3.5 ks and limiting the sensitivity of the observations.

At GeV energies, *Fermi*-LAT (Atwood et al. 2009) proved to be efficient in detecting SNRs (Acero et al. 2015, 2016; Ackermann et al. 2016). Above 100 MeV, two populations of SNRs seem to be emerging: a population of young, X-ray bright, SNRs (Abdo et al. 2011; Tanaka et al. 2011) and a second one including evolved GeV-bright SNRs, interacting with MCs (Reichardt et al. 2012; Abdo et al. 2010). SNR G24.7+0.6 belongs to the latter group. Although initially associated with the pointlike source 3FGL J1833.9–0711, SNR G24.7+0.6 appears in the first *Fermi* SNR catalog (Acero et al. 2016) as an extended source ($\mathrm{TS_{ext}} = 24.89$) with a gaussian morphology of radius $0.25° \pm 0.04°_{\mathrm{stat}} \pm 0.12°_{\mathrm{sys}}$ centered at $\mathrm{RA_{J2000}} = 278.60° \pm 0.03°_{\mathrm{stat}} \pm 0.1°_{\mathrm{sys}}$ and $\mathrm{DEC_{J2000}} = -7.17° \pm 0.03°_{\mathrm{stat}} \pm 0.03°_{\mathrm{sys}}$. The *Fermi*-LAT extension is compatible with the radio size, but offset by 0.08° towards the star-forming region G24.73+0.69. Its extension at energies larger than 10 GeV was confirmed by the presence of the SNR in both the catalog of extended sources in the Galactic plane (FGES, Ackermann et al. (2017)) and the third catalog of hard *Fermi*-LAT sources (3FHL, Ajello et al. (2017)). SNR G24.7+0.6 has been, in fact, identified with FGES J1834.1–0706 and 3FHL J1834.1–0706e. The 3FHL tag confirms the hard spectral nature of the source, thus a potential VHE γ-ray emitter. The spectral results of the sources identified with the SNR G24.7+0.6 are all compatible within each other showing that the energy spectrum is well-represented with a power-law function of index 2.2. We take as reference from now on the spectral results in the FGES catalog (Ackermann et al. 2017): a photon index of 2.28 ± 0.14 and an integral flux from 10 GeV to 2 TeV of $(5.37 \pm 0.66) \times 10^{-10}$ erg cm^{-2} s^{-1}.

Above ~500 GeV, the region was covered by the H.E.S.S. Galactic Plane Survey (HGPS, Deil et al. 2015). The HGPS shows a large and bright source, dubbed HESS J1837–069 (Aharonian et al. 2005, 2006), located 0.9° away (at $\mathrm{RA_{J2000}} = 279.41°$ and $\mathrm{DEC_{J2000}} = -6.95°$) from SNR G24.7+0.6. HESS J1837–069 has an elliptical extension of $0.12° \pm 0.02°$ and $0.05° \pm 0.02°$ (with an orientation angle of the semi-major axis of $\omega = 149° \pm 10°$ counterclockwise with respect to the positive Galactic latitude axis) at energies above 200 GeV. The power-law spectrum of HESS J1837–069 exhibits a photon index of 2.27 ± 0.06 and an integral flux above 200 GeV of $(30.4 \pm 1.6) \times 10^{-12}$cm^{-2}s^{-1}. HESS J1837–069 has been classified as a PWNe, associated to the pulsar PSR J1838–065 (or AX J1838.0–0655) (Gotthelf & Halpern 2008). Deeper observations of the region around HESS J1837–069 (Marandon et al. 2008) led to a more detailed morphological analysis resulting in a new position of HESS J1837–069 offset 0.05° from the initial report at $\mathrm{RA_{J2000}} = 279.37° \pm 0.008°$ and $\mathrm{DEC_{J2000}} = -6.92° \pm 0.008°$ with a size of $0.22° \pm 0.01°$. These observations also revealed a second source located to the South of HESS J1837–069, when considering the International Celestial Reference System (ICRS). No official name was attributed to this potential new source. However, no significant emission from the SNR G24.7+0.6 region was claimed. Recent results from the new HGPS (H.E.S.S. Collaboration et al. 2018) characterise the region of HESS J1837–069 as a superposition of three Gaussian sources with a total extension of $0.36° \pm 0.03°$. This region of the sky was also covered by HAWC at energies above 1 TeV. The second HAWC catalog (Abeysekara et al. 2017) shows a 15σ-excess compatible with the position of HESS J1837–069 after 1.5 year observation time.

In this paper, we study the interesting region centered around SNR G24.7+0.6 with *Fermi*-LAT in the energy range between 60 MeV and 500 GeV. We also explore with the MAGIC telescopes the region around it to investigate the spectral behaviour above 150 GeV in order to constrain the emission region observed by *Fermi*-LAT around the SNR.

2 OBSERVATIONS AND DATA ANALYSIS

2.1 *Fermi*-LAT

We analysed ~8 years of data spanning from 4 August 2008 to 13 June 2016 with energies between 60 MeV and 500 GeV. The dataset was analysed using *Fermipy*[1] v0.13.3: a set of python programmed tools that automatise the PASS8 analysis with the Fermi Science Tools[2]. The CLEAN event class was chosen for this analysis since the source is shown to be extended (Acero et al. 2016). In addition, it benefits from a lower background above 3 GeV with respect to the SOURCE event class. We used P8R2_CLEAN_V6 instrument response function (IRF). This IRF is divided into three event types, FRONT/BACK, PSF and EDISP. For the analysis presented here we used the PSF partition which guarantees the best quality of the reconstructed direction. This PSF partition is subdivided into four quartiles increasing in quality from PSF0 to PSF3, each of which with its zenith angle cut to reduce the background from the Earth limb. Thus photons with zenith angles larger than 70, 75, 85 and 90 for PSFs ranging from the worst to the best were excluded. The analysis of the four quartiles was performed independently and combined in later stages of the analysis by means of a joint likelihood fit.[3]

We performed a maximum likelihood analysis in a circular region of 20° radius centered on the radio source position $\mathrm{RA_{J2000}} = 278.57°$; $\mathrm{DEC_{J2000}} = -7.09°$, this region will be referred as the region of interest (ROI). The emission model for our ROI includes the LAT sources listed in the third LAT catalog (3FGL, Acero et al. 2015) within a region of 30° radius around SNR G24.7+0.6 and the diffuse γ-ray background models; the Galactic diffuse emission modelled by *gll_iem_v06.fits* and the isotropic component by *iso_P8R2_CLEAN_V6_PSFX_v06.txt* (where X identifies the number of the PSF quartile), including the instrumental background and the extragalactic radiation. Sources lying within 4° from the source of interest were fit with all their spectral parameters left free. For sources between 4° and 7° and the Galactic diffuse and isotropic components, only the normalisation parameters were allowed to vary. All the spectral parameters for sources located farther than 7° from the source of study remained fixed in the maximum likelihood fit.

Due to strong contamination from diffuse emission in the Galactic plane at low energies and the large PSF, both mainly below 1 GeV, in order to study the morphology of the source we performed a specific analysis to the LAT data above 1 GeV in a 8°×8° region centered on the SNR G24.7+0.6 radio position. Given that our source of interest might be associated with two 3FGL sources (3FGL J1834.6–0659 and 3FGL J1833.9–0711), which are tagged as 'confused', meaning that they can arise from a wrongly modeled background or a confused source pile-up, we removed them from the model to study in more detail the residual map. We found that replacing these sources with a single point-like source (we called it FGES J1834.1–0706 as in Ackermann et al. 2017) located at the radio position increases the likelihood value. We performed a *localisation procedure*[4] within a region of 3°×3° to determine the correct position of FGES J1834.1–0706 and we tested for a possible extended morphology modeling our source with a Gaussian function rather than a point-like source. Assuming a power-law spectral shape with spectral index -2, we performed an iterative likelihood fit for values of the source extension[5] ranging from 0.01° to 1.01° with a step of 0.1°.

To obtain the spectral energy distribution, we split the 60 MeV–500 GeV energy range into 10 logarithmically spaced bins. Each spectral point has at least a TS value

[1] http://fermipy.readthedocs.io/en/latest/
[2] https://fermi.gsfc.nasa.gov/ssc/data/analysis/documentation/
[3] http://fermipy.readthedocs.io/en/latest/fitting.html
[4] http://fermipy.readthedocs.io/en/latest/advanced/localization.html
[5] http://fermipy.readthedocs.io/en/latest/advanced/extension.html

greater than or equal to 4, otherwise 95% confidence level (CL) flux ULs were computed.

2.2 MAGIC telescopes

The VHE γ-ray observations of SNR G24.7+0.6 were performed using the MAGIC telescopes. MAGIC observed SNR G24.7+0.6 between April 5th and August 29th, 2014, for a total of 33 hours, at zenith angles between 35° and 50°, yielding an analysis energy threshold of ~200 GeV. The observations were performed in wobble-mode (Fomin et al. 1994) at four symmetrical positions 0.4° away from the source, so that the background can be estimated simultaneously. After quality cuts, which account for hardware problems, unusual background rates and reduced atmospheric transparency, 31 hours of high quality data were selected.

The analysis of the MAGIC data was performed using the standard MAGIC Analysis and Reconstruction Software, MARS (Moralejo et al. 2010; Zanin et al. 2013). In particular, we derived On-maps of γ-like events based on their arrival directions in sky coordinates. ON-maps need a reliable background determination in order to minimize the contribution of hadronic cosmic rays surviving data selection cuts. To reconstruct the background maps from wobble observations we use the Exclusion Map technique implemented in SkyPrism (Vovk et al. 2018). The Exclusion Map technique allows to estimate the background with no need of prior knowledge of the position of the source under evaluation while we exclude from the computation regions containing known sources. ON and Background maps are used as input files for a two-dimensional maximum likelihood fit of the source model that is performed using the *Sherpa* package (Doe et al. 2007; Freeman et al. 2001). Specifically, the source model is constructed and optimized by using an iterative method in a likelihood approach. First, a single Gaussian-shaped source is added to a model containing only the isotropic background. Different positions and extensions of the source are evaluated and the values maximising the likelihood value are assigned to the source. A second Gaussian-shaped source is added to the model and the same procedure is executed; positions and extensions for both sources are re-calculated. These two nested models are compared through their maximum likelihood fit value. Additional Gaussian-shaped sources are iteratively introduced to the model until the maximum likelihood fit is no longer improved. Given the complexity of the region, together with the drop in the sensitivity of MAGIC when one moves away from the center, only symmetric gaussian-type sources could be tested. For the spectral analysis of the best-fit model obtained, we performed an additional one-dimensional maximum likelihood fit using `SkyPrism`.

3 RESULTS

The obtained MAGIC significance skymap, shown in Figure 1 (*left* panel) in the ICRS coordinate system, shows significant extended emission at energies larger than 200 GeV. The two-dimensional likelihood morphological analysis led to the detection of three distinct sources:

- The brightest source is identified with HESS J1837–069 (Aharonian et al. 2006; Marandon et al. 2008). It presents an extended morphology characterized by a symmetric Gaussian of 0.23° ±0.01° size centered at RA_{J2000}=279.26° ±0.02° and DEC_{J2000}=−6.99° ± 0.01°. This emission is also associated with the extended source FGES J1836.5–0652 in the *Fermi*-LAT catalog of extended sources in the Galactic plane.
- The excess to the South from HESS J1837–069 is significantly detected with a peak significance of 8.2σ. We added a new point-like source in our morphological model of the region to account for this excess. The two-sources model is favoured with respect to the one-single-source one at 7.7σ level. This new source is well-fit with a Gaussian shape with an extension of 0.08° ± 0.05° centered at RA_{J2000} = 279.34° ± 0.14° and DEC_{J2000} = −7.28° ± 0.24°. The comparison between a model describing the source as point like and a model treating the source as a Gaussian results in a ΔTS of 23 or ~5σ, favouring the second model to describe the total emission. Spatially coincident with the hotspot reported in Marandon et al. (2008), we named it MAGIC J1837–073 since no name was officially previously attributed to it. This source is also coincident with 3FGL J1837.6–0717 reported in the Third Catalog of *Fermi*-LAT sources (Acero et al. 2015).
- The third significant source (with a peak significance of 11.0σ) is, for the first time, detected at VHE, and it is named MAGIC J1835–069. The source is resolved at a level of 13.5σ when adding it to the global fit. It is significantly extended and well modelled by a Gaussian of 0.21° ± 0.05° centered at RA_{J2000} = 278.86° ± 0.23° and DEC_{J2000} = −6.94° ± 0.05°. The extended nature of the source is favoured at a level of 7.1σ. Its center position is offset by 0.34° with respect to the center of the SNR G24.7+0.6. In particular, it lies between two extended sources detected above 10 GeV by *Fermi*-LAT, FGES J1836.5–0652 and the FGES J1834.1– 0706, being the first associated to HESS J1837–069 and the second to the SNR G24.7+0.6.

Figure 2 shows the SED obtained for the three sources with the likelihood method explained in Section 2.2 and using the above-described morphologies as extraction regions. The spectral fit parameters are summarized in Table 1. The differential energy spectrum of HESS J1837–069 is well represented by a power-law function with a photon index of 2.29 ± 0.04 and an integral flux above 200 GeV of (7.2 ± 0.3) × 10^{-11} erg cm^{-2} s^{-1}. The spectrum obtained is compatible within statistical errors with those measured by H.E.S.S., 2.27 ± 0.06 in Aharonian et al. (2006) and 2.34 ± 0.04 in Marandon et al. (2008). For MAGIC J1837–073, the best spectral fit model is a power-law with a 2.29 ± 0.09 photon index and an integral flux above 200 GeV of (1.5 ± 0.1) × 10^{-11} erg cm^{-2} s^{-1}. The emission fades away above 3 TeV, and the calculated 95% CL UL at 6 TeV does not constrain any potential cut-off. Finally, the energy spectrum of MAGIC J1835–069 is best fit by a power-law function with a photon index of 2.74 ± 0.08 and an integral flux above 200 GeV of (4.4 ± 0.6) × 10^{-11} erg cm^{-2} s^{-1}.

The results obtained with our *Fermi*-LAT analysis are in good agreement with previously published ones. Two sources are detected in the surrounding of SNR G24.7+0.6; FGES J1834.1–0706 and the counterpart of the MAGIC source MAGIC J1837–073, 3FGL J1837.6–0717. The first

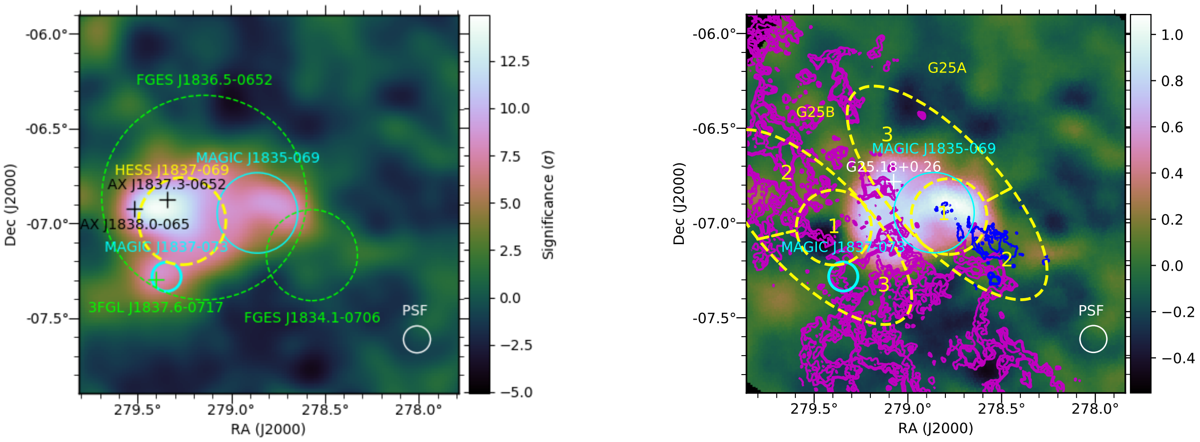

Figure 1. *Left:* $2^{\circ} \times 2^{\circ}$ significance map of the region obtained with MAGIC. The extension of MAGIC J1835–069 and MAGIC J1837–073 are represented by the thin and thick blue circles, respectively, while *Fermi*-LAT sources from FGES and 3FGL catalogs in the FoV are displayed by green dashed lines and a cross. The position and extension of HESS J1837–069 as measured in this work are displayed by a yellow dashed circle. The positions of the two X-ray PWN candidates in Gotthelf & Halpern (2008) are marked with black crosses. AX J1838.0–0655 is proposed as counterpart of HESS J1837–069. *Right:* Residual map (data-model) in counts normalised to 1 derived from MAGIC data after subtracting the emission from HESS J1837–069 and MAGIC J1837–073. Over the MAGIC map, the SNR G24.7+0.6 radio emission and ^{13}CO contours are overlaid in blue and magenta, respectively. The integrated in all velocities ^{13}CO (J=1-0) contours from the Galactic Ring Survey are selected from 7 K to 13 K in step of size 3 to emphasise the cloud spacial distribution. The yellow dashed ellipses (G25A and G25B) along with their three components represent the *Fermi*-LAT sources found within the region by Katsuta et al. (2017). The white cross displays the position of the OB association/cluster G25.18+0.26 identified through X-ray observation by Katsuta et al. (2017).

shows an extended Gaussian emission of $0.24^{\circ} \pm 0.01^{\circ}$ centered at $\mathrm{RA_{J2000}} = 278.57^{\circ} \pm 0.01^{\circ}$ and $\mathrm{DEC_{J2000}} = -7.19^{\circ} \pm 0.02^{\circ}$, offset by 0.1° from the radio position. The significance of the extension is of 11.4σ ($\mathrm{TS_{ext}} = 131$[6]). This result is in agreement with the one published in the FGES catalog. As stated in Section 1, we consider as reference analysis the one of the FGES catalog, thus we refer to the source found in our analysis as FGES J1834.1– 0706.

The energy spectra obtained with our *Fermi*-LAT analysis from 60 MeV to 500 GeV for FGES J1834.1–0706 and MAGIC J1837–073 are represented in Figure 2. MAGIC J1837–073, for which we used the morphology derived in the MAGIC analysis, exhibits a power-law spectrum with a photon index of $\Gamma = (2.15 \pm 0.05)$ and a normalisation factor of $N_0 = (3.9 \pm 0.4) \times 10^{-8}\,\mathrm{TeV^{-1}\,cm^{-2}\,s^{-1}}$ at the decorrelation energy of 8 GeV. The mismatch between the flux level obtained by the two instruments is well within the systematic uncertainties, estimated to be of the order of 15% for MAGIC. A joint χ^2 fit of MAGIC J1837–073 between 60 MeV and 10 TeV results in a similar power-law of photon index $\Gamma_{joint} = (2.12 \pm 0.02)$ with a factor of $N_0 = (1.52 \pm 0.1) \times 10^{-12}\,\mathrm{TeV^{-1}\,cm^{-2}\,s^{-1}}$ at 1 TeV. On the other hand, FGES J1834.1– 0706 shows a power-law spectrum with a photon index of $\Gamma = (2.14 \pm 0.02)$ and a normalisation factor of $N_0 = (2.9 \pm 0.1) \times 10^{-7}\,\mathrm{TeV^{-1}\,cm^{-2}\,s^{-1}}$ at the decorrelation energy of 5.8 GeV. In this case, the energy spectrum of FGES J1834.1– 0706 connects smoothly with that of MAGIC J1835–069 even though the extraction regions are not exactly the same, thus suggesting that the two

[6] It was calculated from $\mathrm{TS_{ext}} = \mathrm{TS_{gauss}} - \mathrm{TS_{point}}$ as stated in Lande et al. (2012)

Table 1. Fitting spectral parameters of the three sources detected by MAGIC. Γ is the photon index, and F_0 the normalisation factor at the decorrelation energy E_0.

	F_0 [$\mathrm{TeV^{-1}\ cm^{-2}\ s^{-1}}$]	Γ	E_0 [TeV]
HESS J1837–069	$(4.4 \pm 0.2) \times 10^{-12}$	2.29 ± 0.04	1.25
MAGIC J1837–073	$(1.7 \pm 0.1) \times 10^{-12}$	2.29 ± 0.09	0.95
MAGIC J1835–069	$(1.4 \pm 0.2) \times 10^{-12}$	2.74 ± 0.08	1.31

Table 2. Joint χ^2 fit spectral parameters for SNR G24.7+0.6 from 60 MeV to ~10 TeV. Photon index, Γ, normalisation factor F_0 at the decorrelation energy E_0 and cutoff energy are presented.

	F_0 [$\mathrm{TeV^{-1}\ cm^{-2}\ s^{-1}}$]	Γ	E_C [TeV]	E_0 [GeV]
EPWL	$(9.1 \pm 3.0) \times 10^{-10}$	2.12 ± 0.02	1.9 ± 0.5	92

sources most likely have a common origin. Under this assumption, we performed a joint χ^2 fit between 60 MeV and 10 TeV that resulted in a power-law function with an exponential cut-off (hereafter, EPWL), $F_0 \left(\frac{E}{E_0}\right)^{-\Gamma} e^{-\frac{E}{E_c}}$, where F_0 is the prefactor; E_0 is the decorrelation energy; E_c is the cut-off energy and Γ is the photon index. The resulting fitting parameters are provided in Table 2.

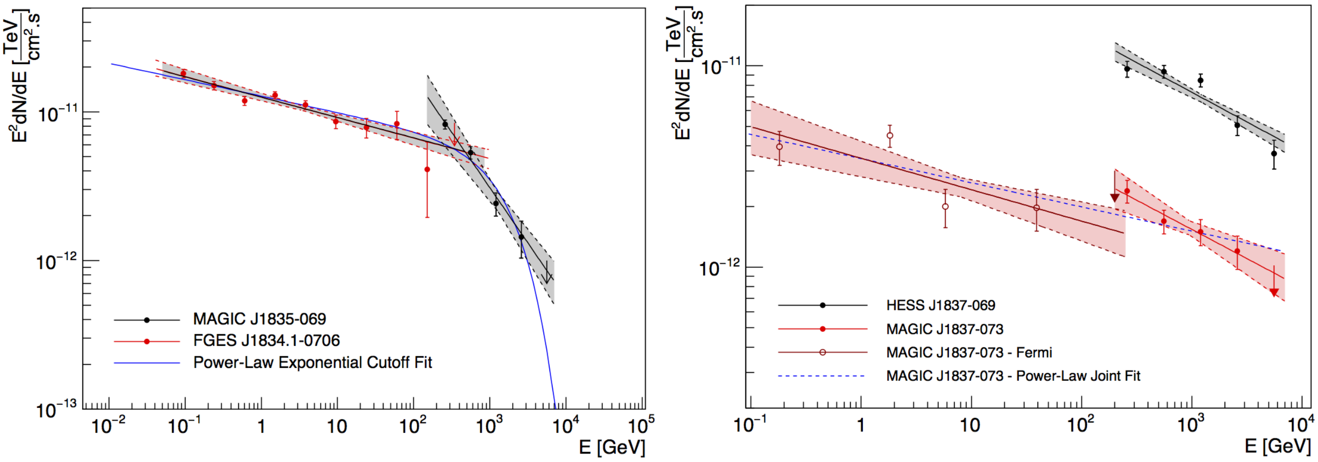

Figure 2. *Left:* Spectral energy distribution of FGES J1834.1–0706 (red circles) and MAGIC J1835–069 (black circles) between 60 MeV and 10 TeV obtained with the analysis described in Section 2.2. In the *Fermi* energy range the spectrum follows a power-law of index 2.14 while it softens in the MAGIC range to an index of 2.74. The EPWL fit for the whole energy range is represented by a blue line. Light gray bands are the statistical uncertainties. *Right:* Spectral energy distribution of HESS J1837–069 (black) and MAGIC J1837–073 (red), measured by MAGIC between 200 GeV and 10 TeV. Solid lines represent the power-law fits applied to each spectrum. Light shaded bands are the statistical uncertainties. The spectrum measured for MAGIC J1837–073 with *Fermi*-LAT along with its power-law fit is represented in dark red. Blue dashed line represents the joint χ^2 fit of MAGIC J1837–073 between 60 MeV and 10 TeV.

4 DISCUSSION

We observed the FoV of SNR G24.7+0.6 with the MAGIC telescopes, following the detection of a hard-spectrum source reported by the LAT collaboration (Ackermann et al. 2016), coincident with the position of the remnant. The analysis of 31 hours of data using the *Sherpa* package on the reconstructed skymap resulted in the detection of three different sources in the MAGIC data set. The brightest one, located at RA_{J2000}=279.26° ± 0.02° and DEC_{J2000}=−6.99° ± 0.01°, has been previously reported by the H.E.S.S. collaboration and namedHESS J1837–069. It is classified as PWNe based on the detailed spectral-morphological study performed by the H.E.S.S. collaboration and the discovery of the associated X-ray source AX J1838.0–0655 (Gotthelf & Halpern 2008). The spectral features derived by MAGIC in this region are compatible within errors with those reported by H.E.S.S.

To the South, MAGIC J1837–073, a γ-ray excess located 0.34° away from HESS J1837–069 is detected at a level of 7.7σ. The spectrum of this source extends to low energies. The origin of this emission remains unclear, although, under a first approximation assumption of one single parent population, an hadronic scenario is most likely to explain a single power-law spectrum up to few tens of TeV. The region was subject of observations with *XMM*-Newton (Katsuta et al. 2017) in a search for a multi-wavelength counterpart of the GeV emission they detect (G25B in Figure 1, *right* panel). No PWN, SNR, or pulsar with spin-down luminosity $> 1\times10^{34}$ erg s^{-1} was found in the region. However, the region is rich in molecular content at velocities $v = 45 - 65$ km s^{-1}. In the GeV regime, it has been postulated as possible association with a bubble identified with the stellar cluster candidate G25.18+0.26, but no sign of such connection can be derived from the TeV data. If, based on the spectral shape and the presence of molecular target, we assume an hadronic origin of the emission (Katsuta et al. 2017). The total luminosity of MAGIC J1837–073 above 100 MeV will amount to $L_\gamma = 1.3\times10^{35}$ erg s^{-1}, for a distance of $d = 5$ kpc. This implies a total cosmic rays energy of $W_p \approx 2.1\times10^{50}\,\mathrm{erg}\left(\frac{\mathrm{cm}^{-3}}{n}\right)$, being n the ambient proton density. This number is comparable to the ones found in other clusters such Westerlund 2 (Yang et al. 2018) or Cygnus Cocoon (Ackermann et al. 2011). Such large luminosity could be achieved by assuming a quasi-continuous injection of cosmic rays, powered by the kinetic energy released for instance in the winds of massive stars ($\sim 1\times10^{38}$ erg s^{-1}), integrating during the cluster lifetime (typically $\sim 1\times10^4$ yrs).

Finally, the statistical test performed allows to resolve MAGIC J1835–069 ($\mathrm{RA_{J2000}}$ = 278.86° ± 0.23°; $\mathrm{DEC_{J2000}}$ = −6.94° ± 0.05°) from HESS J1837–069 at a 13.5σ level. Moreover, the projected distance of the new γ-ray enhancement to the pulsar associated to HESS J1837–069 (for a distance of 6.6 kpc, from Gotthelf & Halpern (2008)), is more than ~65 pc, which, if not impossible, makes the association between the two sources unlikely. MAGIC J1835–069, however, partially overlaps with the emission detected with *Fermi*-LAT (see Figure 1 and Figure 3 for a zoom in of the region). Indeed, a new analysis presented by Ackermann et al. (2017) describes the complex region with three very extended sources, being the MAGIC source comprised between two sources; FGES J1836.5–0652, which includes also HESS J1837–069, and FGES J1834.1–0706 which is consistent with 3FHL J1834.1–0706e on the position of the SNR G24.7+0.6. The flux measured with MAGIC is in good agreement with the one measured by LAT, extending the spectrum from 60 MeV to 10 TeV with a spectral photon index of ~2.74. The VHE broad band spectral shape shows a clear break in the GeV-TeV regime. This change of slope can be described by a power-law with an exponential cut-off at $\mathrm{E_C}$ = 1.9 TeV. The source shows an extended morphology and it is offset 0.34° with respect to center of the remnant, in a region where the later seems to be blowing an IR shell. The measured offset translates onto a projected size of 30 pc at the distance of 5 kpc. The CO-rich surrounding of SNR G24.7+0.6 could be originating the detected GeV-TeV

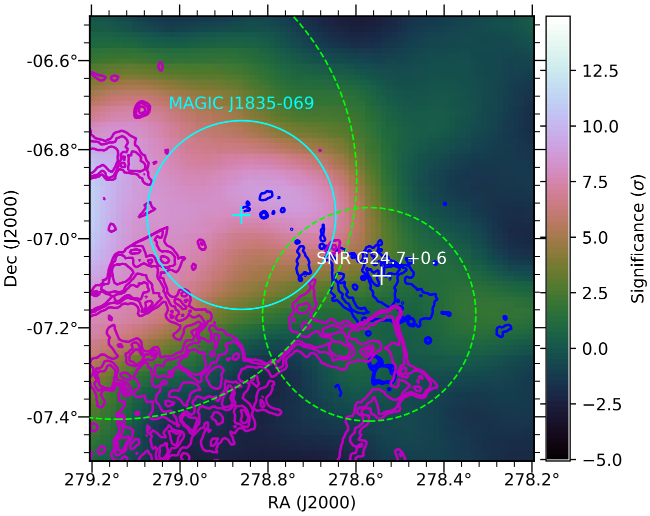

Figure 3. $1° \times 1°$ significance map of the region obtained with MAGIC. MAGIC J1835–069 is marked with a blue line. The green circles show the extension of the *Fermi*-LAT sources from FGES catalog. The VLA radio contours of the region are overlaid in blue, showing the extension of SNR G24.7+0.6 centered at the position of the white cross. The integrated ^{13}CO ($J = 1 \rightarrow 0$) intensity contours from the Galactic Ring Survey are showed in magenta[7].

emission, and the offset between the emission detected by LAT and the MAGIC source could be interpreted in terms of diffusion mechanism similar to what was proposed for IC 443 (Torres et al. 2008, 2010), since the diffusion radius of runaway protons of 100 GeV could account for this distance. However the large error in the position and the complexity of the region in the GeV and TeV regime prevent further conclusions in that sense. Nevertheless, in this scenario and similarly to other evolved SNR, the VHE LAT/MAGIC combined spectrum model can be explained as a result of proton-proton interaction between the cosmic rays accelerated in SNR G24.7+0.6 and those in the surrounding gas. The total luminosity above 100 GeV amounts $L_\gamma = 7.5 \times 10^{34}\,\mathrm{erg\,s^{-1}}$, which translates to a total energetics stored in accelerated protons of $W_p = 1.3 \times 10^{50}\,\mathrm{erg}\left(\frac{\mathrm{cm}^{-3}}{n}\right)$.

A second scenario involving a yet-undiscovered PWN associated to the remnant cannot be discarded. At a distance of d~5 kpc, the separation between MAGIC J1835–069 and the position of the remnant is within the range of offsets found in VHE PWNe (see Figure 6 from H. E. S. S. Collaboration et al. 2018). The corresponding surface brightness, in the energy range from 1 to 10 TeV, would be $\sim 1.2 \times 10^{30}\,\mathrm{erg\,s^{-1}\,pc^{-2}}$. Applying the correlation found by H. E. S. S. Collaboration et al. (2018) (S~ $\dot{E}^{0.81\pm0.14}$), an extremely bright $\dot{E} \sim 1.4 \times 10^{37}\,\mathrm{erg\,s^{-1}}$ pulsar should be powering the VHE source. Both the upper and the lower limit of the spin-down luminosity (S~ $\dot{E}^{0.67}$ and S~ $\dot{E}^{0.95}$, respectively) seem unrealistically large for not being detected either in γ-ray or radio. However, the strong confusion due to the several extended sources in the field limits the detection of such pulsars in the GeV regime. In addition, the extension of the PWN would exceed the SNR size, rendering this scenario unlikely if the putative PWN is connected to the SNR.

Recently, Katsuta et al. (2017) carried out a study of the γ-ray emission coming from the region around, $\mathrm{RA_{J2000}} = 279.22°$ and $\mathrm{DEC_{J2000}} = -7.05°$, with the *Fermi*-LAT telescope. They found that the emission detected is divided into two elliptical extended region, G25A and G25B, composed of 3 components each (see Figure 1, *right* panel). For G25A, all three components have the same spectral shapes while for G25B, the G25B1 component has a harder spectrum than the other two. Due to their elongated morphology and spectral similarity (similar surface brightness and hard energy spectra; $\Gamma = (2.14 \pm 0.02)$ and $\Gamma = (2.11 \pm 0.04)$, respectively), they suggested that both γ-ray emissions are produced by the same astrophysical object. In addition, through X-ray observations of the region with *XMM*-Newton they found the candidate young massive OB association/cluster, G25.18+0.26 (Figure 1, *right* panel). They proposed that both extended γ-ray emissions (G25A and G25B) are associated with an star forming region driven by G25.18+0.26. Assuming the scenario proposed by Katsuta et al. (2017) in which either the accelerated particles are interacting with regions of enhanced gas density or particles are being accelerated within these regions, current TeV telescopes like MAGIC should reveal a diffuse γ-ray emission from the whole G25A and G25B regions. However, as seen from the maps, MAGIC only detects emission from the G25A1 component that is coincident with MAGIC J1835–069. We can conclude it is unlikely that the emission detected at VHE with MAGIC comes from the OB association/cluster G25.18+0.26 detected in X-rays.

5 CONCLUSIONS

MAGIC observations of the field of view of the SNR G24.7+0.6 resulted in the discovery of a new TeV source in the Galactic plane, MAGIC J1835–069, detected above ~150 GeV. The position of MAGIC J1835–069 is compatible at 1.5σ with the center of SNR, which is in turn associated with the *Fermi* source FGES J1834.1–0706. Based on the good agreement between the LAT and MAGIC spectral measurements, the two sources are likely to be associated. The link with the SNR is also plausible if one consider the diffusion radius of particles to explain the observed offset. The GeV-TeV emission observed by *Fermi* and MAGIC can be interpreted as cosmic rays accelerated within the remnant interacting via proton-proton collisions with the ^{13}CO surrounding medium.

A second statistically significant detection of a slightly extended γ-ray signal from the south of HESS J1837–069 is reported. The spectrum of the source extends to 3 TeV with no sign of an spectral break. Although the PWN scenario cannot be ruled out, this detection is believed to be produced by cosmic rays interacting with a stellar cluster. If the latter is confirmed, MAGIC J1837–073 will be part of the scarcely populated group of similar objects like Westerlund 1 and 2 or the Cygnus cocoon and may contribute to a

[7] obtained from https://www.bu.edu/galacticring/new_data.html

better understanding of whether these objects can account for the Galactic cosmic ray flux.

ACKNOWLEDGEMENTS

We would like to thank the Instituto de Astrofísica de Canarias for the excellent working conditions at the Observatorio del Roque de los Muchachos in La Palma. The financial support of the German BMBF and MPG, the Italian INFN and INAF, the Swiss National Fund SNF, the ERDF under the Spanish MINECO (FPA2015-69818-P, FPA2012-36668, FPA2015-68378-P, FPA2015-69210-C6-2-R, FPA2015-69210-C6-4-R, FPA2015-69210-C6-6-R, AYA2015-71042-P, AYA2016-76012-C3-1-P, ESP2015-71662-C2-2-P, CSD2009-00064), and the Japanese JSPS and MEXT is gratefully acknowledged. This work was also supported by the Spanish Centro de Excelencia "Severo Ochoa" SEV-2012-0234 and SEV-2015-0548, and Unidad de Excelencia "María de Maeztu" MDM-2014-0369, by the Croatian Science Foundation (HrZZ) Project IP-2016-06-9782 and the University of Rijeka Project 13.12.1.3.02, by the DFG Collaborative Research Centers SFB823/C4 and SFB876/C3, the Polish National Research Centre grant UMO-2016/22/M/ST9/00382 and by the Brazilian MCTIC, CNPq and FAPERJ.

REFERENCES

Abdo A. A., et al., 2010, ApJ, 712, 459
Abdo A. A., et al., 2011, ApJ, 734, 28
Abeysekara A. U., et al., 2017, ApJ, 843, 40
Acero F., et al., 2015, ApJS, 218, 23
Acero F., et al., 2016, ApJS, 224, 8
Ackermann M., et al., 2011, Science, 334, 1103
Ackermann M., et al., 2016, ApJS, 222, 5
Ackermann M., et al., 2017, ApJ, 843, 139
Aharonian F., et al., 2005, Science, 307, 1938
Aharonian F., et al., 2006, ApJ, 636, 777
Ajello M., et al., 2017, ApJS, 232, 18
Albert J., et al., 2007, ApJ, 664, L87
Aleksić J., et al., 2012, A&A, 541, A13
Atwood W. B., et al., 2009, ApJ, 697, 1071
Deil C., Brun F., Carrigan S., Chaves R., Donath A., Gast H., Marandon V., Terrier R., 2015, in 34th International Cosmic Ray Conference (ICRC2015). p. 773
Doe S., et al., 2007, in Shaw R. A., Hill F., Bell D. J., eds, Astronomical Society of the Pacific Conference Series Vol. 376, Astronomical Data Analysis Software and Systems XVI. p. 543
Fomin V. P., Stepanian A. A., Lamb R. C., Lewis D. A., Punch M., Weekes T. C., 1994, Astroparticle Physics, 2, 137
Freeman P., Doe S., Siemiginowska A., 2001, in Starck J.-L., Murtagh F. D., eds, Proc. SPIEVol. 4477, Astronomical Data Analysis. pp 76–87 (arXiv:astro-ph/0108426), doi:10.1117/12.447161
Gotthelf E. V., Halpern J. P., 2008, ApJ, 681, 515
H. E. S. S. Collaboration et al., 2018, A&A, 612, A2
H.E.S.S. Collaboration et al., 2018, A&A, 612, A1
Jackson J. M., et al., 2006, ApJS, 163, 145
Katsuta J., Uchiyama Y., Funk S., 2017, ApJ, 839, 129
Lande J., et al., 2012, ApJ, 756, 5
Leahy D. A., 1989, A&A, 216, 193
Marandon V., Djannati-Atai A., Terrier R., Puehlhofer G., Hauser D., Schwarzburg S., Horns D., 2008, in Aharonian F. A., Hofmann W., Rieger F., eds, American Institute of Physics Conference Series Vol. 1085, American Institute of Physics Conference Series. pp 320–323, doi:10.1063/1.3076671
Moralejo R. A., et al., 2010, MARS: The MAGIC Analysis and Reconstruction Software, Astrophysics Source Code Library (ascl:1011.004)
Petriella A., Paron S., Giacani E., 2008, Boletin de la Asociacion Argentina de Astronomia La Plata Argentina, 51, 209
Petriella A., Paron S., Giacani E., 2010, Boletin de la Asociacion Argentina de Astronomia La Plata Argentina, 53, 221
Petriella A., Paron S. A., Giacani E. B., 2012, A&A, 538, A14
Reich W., Furst E., Sofue Y., 1984, A&A, 133, L4
Reichardt I., de Oña-Wilhelmi E., Rico J., Yang R., 2012, A&A, 546, A21
S. Longair M., 1992, High Energy Astrophysics. Cambridge University Press
Seward F. D., 1990, ApJS, 73, 781
Tanaka T., et al., 2011, ApJ, 740, L51
Torres D. F., Rodriguez Marrero A. Y., de Cea Del Pozo E., 2008, MNRAS, 387, L59
Torres D. F., Marrero A. Y. R., de Cea Del Pozo E., 2010, MNRAS, 408, 1257
Vovk I., Strzys M., Fruck C., 2018, *In preparation*
Yang R.-z., de Oña Wilhelmi E., Aharonian F., 2018, A&A, 611, A77
Zanin R., Carmona E., Sitarek J., Colin P., 2013, International Cosmic Ray Conference, 1, 773

[1] Inst. de Astrofísica de Canarias, E-38200 La Laguna, and Universidad de La Laguna, Dpto. Astrofísica, E-38206 La Laguna, Tenerife, Spain
[2] Università di Udine, and INFN Trieste, I-33100 Udine, Italy
[3] National Institute for Astrophysics (INAF), I-00136 Rome, Italy
[4] ETH Zurich, CH-8093 Zurich, Switzerland
[5] Università di Padova and INFN, I-35131 Padova, Italy
[6] Technische Universität Dortmund, D-44221 Dortmund, Germany
[7] Croatian MAGIC Consortium: University of Rijeka, 51000 Rijeka, University of Split - FESB, 21000 Split, University of Zagreb - FER, 10000 Zagreb, University of Osijek, 31000 Osijek and Rudjer Boskovic Institute, 10000 Zagreb, Croatia.
[8] Saha Institute of Nuclear Physics, HBNI, 1/AF Bidhannagar, Salt Lake, Sector-1, Kolkata 700064, India
[9] Max-Planck-Institut für Physik, D-80805 München, Germany
[10] now at Centro Brasileiro de Pesquisas Físicas (CBPF), 22290-180 URCA, Rio de Janeiro (RJ), Brasil
[11] Unidad de Partículas y Cosmología (UPARCOS), Universidad Complutense, E-28040 Madrid, Spain
[12] University of Łódź, Department of Astrophysics, PL-90236 Łódź, Poland
[13] Deutsches Elektronen-Synchrotron (DESY), D-15738 Zeuthen, Germany
[14] Institut de Física d'Altes Energies (IFAE), The Barcelona Institute of Science and Technology (BIST), E-08193 Bellaterra (Barcelona), Spain
[15] Università di Siena and INFN Pisa, I-53100 Siena, Italy
[16] Università di Pisa, and INFN Pisa, I-56126 Pisa, Italy
[17] Universität Würzburg, D-97074 Würzburg, Germany
[18] Finnish MAGIC Consortium: Tuorla Observatory and Finnish Centre of Astronomy with ESO (FINCA), University of Turku, Vaisalantie 20, FI-21500 Piikkiö, Astronomy

Division, University of Oulu, FIN-90014 University of Oulu, Finland
[19] Departament de Física, and CERES-IEEC, Universitat Autónoma de Barcelona, E-08193 Bellaterra, Spain
[20] Universitat de Barcelona, ICC, IEEC-UB, E-08028 Barcelona, Spain, E-mail: dgalindo@fqa.ub.edu
[21] Japanese MAGIC Consortium: ICRR, The University of Tokyo, 277-8582 Chiba, Japan; Department of Physics, Kyoto University, 606-8502 Kyoto, Japan; Tokai University, 259-1292 Kanagawa, Japan; RIKEN, 351-0198 Saitama, Japan
[22] Inst. for Nucl. Research and Nucl. Energy, Bulgarian Academy of Sciences, BG-1784 Sofia, Bulgaria
[23] Humboldt University of Berlin, Institut für Physik D-12489 Berlin Germany
[24] also at Dipartimento di Fisica, Università di Trieste, I-34127 Trieste, Italy
[25] also at Port d'Informació Científica (PIC) E-08193 Bellaterra (Barcelona) Spain
[26] also at INAF-Trieste and Dept. of Physics & Astronomy, University of Bologna
[27] Institute for Space Sciences (ICE, CSIC), E-08193 Barcelona, Spain, E-mail: wilhelmi@ice.csic.es
[28] Institut d'Estudis Espacials de Catalunya (IEEC), 08034 Barcelona, Spain
[29] AvH Guest at Deutsches Elektronen Synchrotron DESY, 15738 Zeuthen, Germany
[30] Institució Catalana de Recerca i Estudis Avancats (ICREA), E-08010 Barcelona, Spain
[31] Max-Planck-Institut für Kernphysik, D-69029 Heidelberg, Germany, E-mail: roberta.zanin@mpi-hd.mpg.de